Dalton Transactions

Accepted Manuscript

ROYAL SOCIETY OF CHEMISTRY

www.rsc.org/dalton

Dalton Transactions

RSCPublishing

ARTICLE

A remarkable effect of *N*,*N*-diethylamino functionality on the optoelectronic properties of a salicylimine-based probe for Al^{3+}

Cite this: DOI: 10.1039/x0xx00000x

Received 00th January 2012,
Accepted 00th January 2012

DOI: 10.1039/x0xx00000x

www.rsc.org/

Neeraj,[‡1] Ajit Kumar,[‡1] Virendra Kumar,[1] Rahul Prajapati,[1] Sharad Kumar Asthana,[1] K. K. Upadhyay,[1*] Jianzhang Zhao[2]

A new live-cell permeable, fluorescent probe comprised of a simple salicylimine-based Schiff base (**SA1**) has been developed for Al^{3+} with nano-molar sensitivity in aqueous medium. The **SA1** was synthesized through a simple structural modification of a recently reported receptor **SA2** by the incorporation of N,N-diethylamino (**DEA**) group as a fine controllable unit. This modification affects the performance of SA1 remarkably in terms of its sensitivity, water compatibility, efficiency as well as its mechanistic aspect. The presence of **DEA** group in **SA1** led to its dual channel emission due to TICT state at the same time its hydrophobic nature was also responsible for controlling the strong hydration of Al^{3+} ion in aqueous medium which ultimately led to high sensitivity of **SA1** for Al^{3+}. The structure of the **SA1** was confirmed by single crystal X–ray diffraction and its binding with Al3+ was studied in detail by UV-visible, fluorescence, ^{1}H NMR spectral studies along with mass determination. The effort of getting single crystal of Al^{3+}–**SA1** led to single crystals of Cl^- /NO_3^- complexes of protonated **SA1** which were fully characterized by their XRD studies.

Introduction

Selective signalling of environmentally and biologically important metal ions has gained spectacular development in the field of supramolecular chemistry **[1]**. The Al^{3+} is one of the major pollutants and has maligned our environment through a number of anthropogenic activities. The frequent use of aluminum foil, cooking utensils and trays for convenience might have led an increase in the Al^{3+} concentration in food **[2]**. Peoples are widely exposed to aluminum due to its widespread use in various fields *viz.,* automotive and aeronautic transports, to packaging, food additives, construction, space industries and aluminum-based pharmaceuticals, etc. **[3]**. Acid rain is one of the prime reason for the leaching of aluminium from soil leading to the free Al^{3+} in the environment and surface water, which is deadly towards flora and fauna **[4]**.

The aluminium is a nonessential element for living systems, since it competes and inhibits the role of several essential elements *viz.* Mg^{2+} (0.066 nm), Ca^{2+} (0.099 nm), and Fe^{3+} (0.064 nm) involved in various biological processes due to its similarities regarding ionic potential **[5]**. Its toxicity hampers not only plant growth but also human nervous system which further led to dementia, Alzheimer's disease, Parkinson's disease, amyotrophic lateral sclerosis, etc. **[6].** Accumulation of excessive amounts of this metal damages the kidney, reduces total bone and matrix causing osteoporosis, osteomalacia etc. **[7]**.

Several methods are available in the literature for the estimation and detection of Al^{3+} but the spectrofluorimetry has attracted significant interest due to to its high signalling ability along with high sensitivity and selectivity and its potential use in biological and environmental researches **[8]**. The strong hydration of Al^{3+} in aqueous medium led its weak coordination ability **[9]** and thus only a few Al^{3+} sensors are available in literature as compared to transition metal ions. So it is a challenging task for chemists specially supramolecular chemists to design a selective and sensitive fluorescent probe for Al^{3+} in aqueous medium. A number of derivatives have been exploited hitherto for fluorescence sensing of Al^{3+}. **[10]**. Most of them contain nitrogen–oxygen-rich coordination environments i.e., hard-base environment due to hard nature of the same **[11]**. The simplicity, cost-effectiveness and water compatibility are always matter of concern for optical probes.

[1]*Department of Chemistry (Centre of Advanced Study), Faculty of Science, Banaras Hindu University, Varanasi-221005, India. E-mail: drkaushalbhu@yahoo.co.in;kku@bhu.ac.in, Tel: +91 542 670 2488.*
[2]*State Key Laboratory of Fine Chemicals, Dalian University of Technology, Dalian 116012, China*

† Electronic supplementary information (ESI) available: ^{1}H NMR, ^{13}C NMR, IR, mass spectrum, XRD related data, UV-visible/fluorescence spectrum of SA1 with various analytes has been given. CCDC 943713, 959758 and 959759. For ESI and crystallographic data in CIF or other electronic format see DOI: 10.1039/b000000x/

‡ These authors contributed equally to this work.

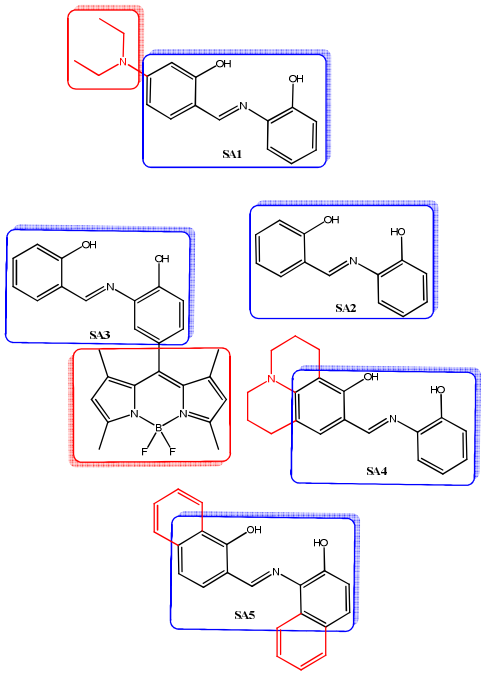

Fig. 1 Fluorescent receptor synthesized by us (SA1) and other workers (SA2-SA5)

The hydrazones and Schiff bases having phenolic –OH groups were found to be most responsive towards Al^{3+} in comparison to other metal ions. Although these types of probes are simple one and employ simple synthetic procedure as well as are cost effective also however most of them suffered from at least one of the following problems i.e., poor detection limit, choice of solvent system and lack of concrete information about the structure of the probe **[12]**. Recently Liu et al. reported the 2-hydroxy-1-napthaldehyde as the simplest fluorescent probe for the selective turn-on fluorescent sensing of Al^{3+} in aqueous solution but with a moderate detection limit of 3.28×10^{-6} only **[13]**. Moreover, a number of other fluorescent receptors for Al^{3+} reported recently are able to work either in organic media or higher amounts of same as a co-solvent with water and thus restrict their practical applications **[14]**.

We herein report an Al^{3+} selective fluorescent probe (**SA1**) obtained by introducing a pendant arm of *N,N*-diethylamino (DEA) group over an earlier reported salicylimine Schiff base (**SA2**) by Kim et al. (Fig. 1) **[15a].** The introduction of DEA over **SA2** serves two purposes firstly it activates the TICT state and secondly introduces local hydrophobicity in **SA1**. Due to TICT state **SA1** fluoresces at two wavelengths 472 and 498 nm simultaneously while hydrophobic nature of DEA group restricts the strong hydration ability of Al^{3+} in aqueous medium and finally led towards its high sensitivity over **SA1**. Receptors with dual emission bands are always preferred due to their high accuracy and precision in terms of analyte sensing **[16]**. The dual emission responsive fluorescent probes for Al^{3+} are still rare in the literature **[14d, 17]**.

Although few other workers also modified **SA2** but all of them are compounded with limitations. Most recently Jiang et al. modified the **SA2** by introduction of 4,4-Difluoro-4-bora-3*a*,4*a*-diaza-*s*-indacene group over **SA2** for getting a yet another Al^{3+} selective fluorescent probe **SA3** (Fig. 1) **[15b]**. The same exhibited strong fluorescence selectivity towards Al^{3+} yet the synthetic procedure adopted for **SA3** was complex one as compared to ours and the same possesses a moderate detection limit of only 1 μM and that too in water containing methanol (v/v = 1:1). Besides these Kim et. al. **[18a]** and Jang et.al **[18b]** reported recently a modified version of **SA2** in the form of receptor **SA4** and **SA5** respectively. The detection limits of both of these receptors were 0.10 μM and 10 μM respectively and hence moderate only. Moreover the synthetic approach of the **SA5** is quite tedious in comparison to that of ours receptor **SA1**. Furthermore the choice of solvents for sensing studies for both **SA4** and **SA5** were also not appreciable for biological applications.

It is worth to mention that our strategy of structural tuning of **SA2** remarkably improved the performance of **SA1** towards Al^{3+} as compared to that of **SA2-SA5**. The, **SA1** possesses better water compatibility, nano-molar sensitivity towards Al^{3+} along with a nice piece of mechanistic pathway supported by spectroscopic, mass spectrometric and single crystal XRD studies. Moreover in terms of detection limit, only a few fluorescent receptors for Al^{3+} with nano-molar sensitivity have been reported in the literature hitherto **[12c, 17a-c, 19]**. Furthermore the 2:1 binding stoichiometry between Al^{3+} and **SA1** is also a rare instance **[19, 20]** in the literature due to its strong hydration and weak coordination ability in comparison to that of transition metal ions **[8]**. Thus the **SA1** being presented by us through present communication was able to overcome most of the problems associated with previously reported Al^{3+} sensors as stated above. The selective recognition of Al^{3+} by **SA1** was explored as the consequence of the combinatorial effects of photoinduced electron transfer (PET), C=N isomerization inhibition, chelation-enhanced fluorescence (CHEF) along with twisted intramolecular charge transfer (TICT) mechanisms.

Experimental

Synthesis of SA1, (E)-5-(diethylamino)-2-(((2-hydroxyphenyl)imino)methyl)phenol

The **SA1** was synthesized by adding 2.0 mM methanolic solution of 4-(diethylamino)-2-hydroxy-benzaldehyde to the equimolar methanolic solution of 2–Amino-phenol followed by boiling under reflux for three hours (Scheme –1). A dark brown crystalline solid was precipitated which was filtered and washed with diethyl ether and finally dried under vacuum over anhydrous $CaCl_2$. The **SA1** was characterized by IR, ^1H & ^{13}C NMR and mass spectral studies **(ESI; Figure S1-S4)** along with its full characterization by single crystal XRD studies.

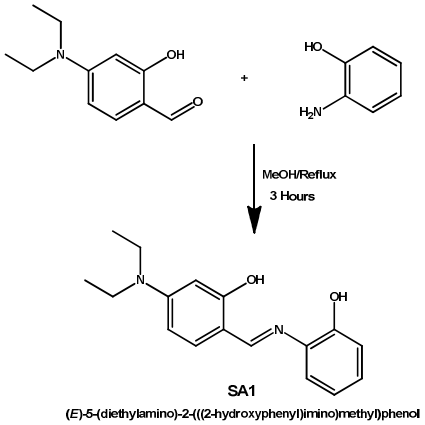

Scheme 1: Synthesis of SA1

Yield: 90%; **IR/cm^{-1}:** 3435, 2976, 2553, 1617, 1595, 1505, 1466, 1410, 1342, 1258, 1229, 1141, 1009, 975, 739, 692, 600, 545, 471, 440; **^{1}H NMR (300 MHz, DMSO-d$_6$, TMS): δ ppm** = 14.19 (s, 1H, –OH), 9.58 (s, 1H, –OH), 8.61 (s, 1H, –CH=N–), 5.91 (s, 1H, Ar–H), 6.22-6.25 (d, 1H, Ar–H), 6.79-7.02 (m, 4H, Ar–H), 7.22-7.26 (t, 1H, Ar–H), 1.13-1.08 (t, 6H, –CH_3), peak for –CH_2 merged with the solvent peak; **^{13}C NMR (75 MHz, DMSO-d$_6$) δ ppm:** 165.960, 158.493, 151.685, 150.061, 134.510, 134.015, 126.185, 119.617, 118.488, 116.188, 109.043, 103.744, 103.611, 97.307, 97.208, 43.901, 12.616; **ESI MS m/z (M+H)**: 285.3. Calc. for $C_{17}H_{20}N_2O_2$ = 284.15.

Synthesis of Al^{3+}complex with SA1

A 10 mL methanolic solution of $AlCl_3$ (0.067g, 0.5 mmol) was added slowly to a magnetically stirred 10 mL methanolic solution of **SA1** (0.142g, 0.5 mmol). The reaction mixture was stirred on ice bath for ~3 h whereby a dark orange ppt. was formed. It was filtered, washed with water several times followed by diethylether and finally dried under vacuum over anhydrous $CaCl_2$. The complex was characterized by IR, ^{1}H & ^{13}C NMR along with mass spectral studies **(ESI; Figure S5-S8)**.

Yield: 85%; **IR/cm^{-1}**: 3391, 3225, 3110, 2982, 2567, 1635, 1610, 1593, 1525, 1463, 1485, 1427, 1347, 1274, 1242, 1142, 1177, 1080, 1009, 959, 839,791,768, 693, 663, 533, 465. **^{1}H NMR (300 MHz, DMSO-d$_6$, TMS): δ ppm** = 11.64 (s, 1H, –NH), 11.02 (s, 1H,–OH), 8.98 (s, 1H, –CH=N–), 6.40 (s, 1H, Ar–H),6.59-6.62 (d, 1H, Ar–H), 6.93-7.19 (m, 4H, Ar–H), 7.59-7.69 (d, 1H, Ar–H), 1.14-1.18 (t, 6H, –CH_3), 3.35-3.50 (–CH_2, 4H); **^{13}C NMR (DMSO-d$_6$, 75 MHz)**: **δ ppm** = 163.858, 155.921, 153.921, 148.018, 127.784, 125.592, 119.609, 116.213, 107.073, 104.741, 96.582, 44.651, 12.286, 12.204. **ESI MS m/z (M$^+$)**: 593.4; Calc. for $[C_{34}H_{38}N_4O_4Al]^{3+}$ = 593.29.

Results and discussion

X-ray crystallographic studies

The structure of **SA1** was confirmed through its single crystal X-ray analysis. Single crystals of **SA1** were obtained by slow evaporation of its saturated DMF–DCM (1:1, v/v) solution. The **SA1** crystallizes into a triclinic lattice with space group P-1. An ORTEP view of the asymmetric unit of **SA1** is shown in Fig. 2 while crystal data and structural refinement details are listed in **ESI: Table 1**.

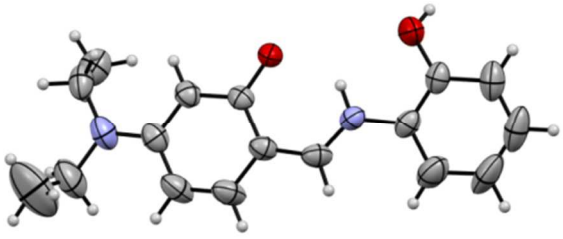

Fig. 2 Single crystal of SA1

The asymmetric unit contains three molecules of the **SA1** with different orientation of the DEA groups (Fig. 3). Among the three molecules two possess *trans* orientation of ethyl groups while remaining one had *cis* orientation. In each molecule, the two benzene rings and azomethine groups are practically coplanar. All the three molecules adopt an (E)-configuration about the C=N bond (C21–N3, C12–N8 and C18–N6) having bond distances 1.308 Å, 1.325 Å and 1.315 Å respectively and are appreciably close to that of a C=N bond (1.30 A°). The hydrogen atoms particularly i.e., N3H, N8H and N6H are localized at aldimine N atom and thus the **SA1** takes tautomeric keto form with the strong intra- and intermolecular N–H----O and O–H----O interactions (Fig. 3). The corresponding bond distances between heavy atoms i.e., N and O involved in hydrogen bondings are found to be 2.694 (N3–O2), 2.593 (O2–O5), 2.639 (N8–O10) and 2.650 (N6–O1) A°. The above structure is further supported by the shortening of the bond O11—C2, C10–C27 and O1-C17 to 1.295, 1.300 and 1.306 A° respectively. On the other hand the bond lengths between C–atom and phenolic O–atoms i.e., O7–C20, O5–C24 and O4–C34 were found to be 1.350 Å, 1.347 Å and 1.352 Å respectively. These observations clearly indicated the presence of only one phenolic –OH group in the crystal structure of **SA1**. While in solution state ^{1}H NMR spectrum of **SA1** in DMSO–d$_6$ enabled the visibility of both phenolic protons i.e., enolic form (**ESI; Figure S1**).

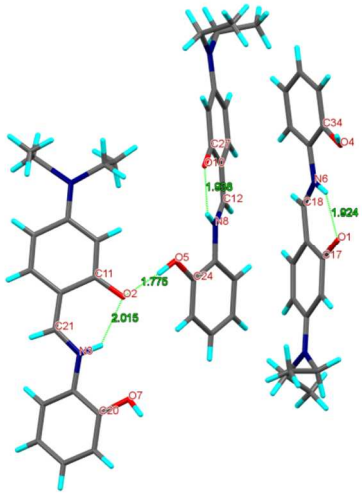

Fig. 3 Showing Intra and intermolecular hydrogen bondings in SA1

The hydrogen bondings in **SA1** enabled nice supramolecular architecture of the same as shown in Fig. 4. The yet another effect of this hydrogen bonding was partial planarity in **SA1** which ultimately led to its weak fluorescent nature by the partial quenching of PET.

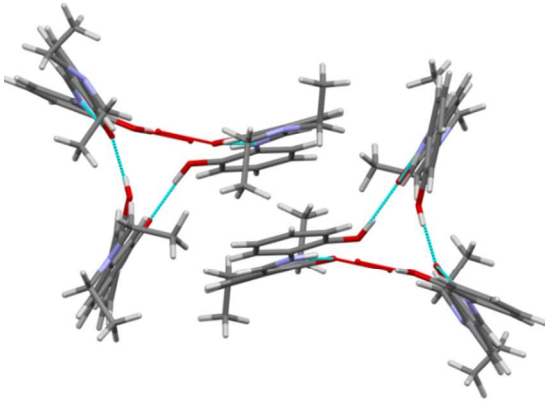

Fig. 4 Formation of supramolecular architecture of SA1 molecule through hydrogen bonding

Photo physical studies of SA1

The spectroscopic properties of the **SA1** were investigated in its 10 μM aqueous solution. As illustrated in Fig. 5, free **SA1** exhibited a strong absorption band centered at 419 nm due to π–π* transitions. The same underwent hypochromic shifting along with a meager red shifting by ~ 5 nm upon concomitant additions of Al^{3+} ion (0–10 equiv.). At this stage the color of the solution became olive green from light yellow (Inset, Fig. 5). Three isosbestic points at 307, 355 and 451 nm further confirmed formation of the **SA1**+Al^{3+} complex. The separate additions of 10 equiv. each of other metal ions *viz.,* Na^{+}, K^{+}, Mg^{2+}, Ba^{2+}, Al^{3+}, Ca^{2+}, Cr^{3+}, Mn^{2+}, Co^{2+}, Ni^{2+}, Zn^{2+}, Cd^{2+}, Hg^{2+} and Pb^{2+} as their chloride salts did not perturb the UV-visible spectral pattern of **SA1** to a significant extent (**ESI; Figure S9**). However Cu^{2+} and Fe^{3+} did affect to a large extent in terms of hypochromic shifting along with broadening of the 419 nm absorption band of **SA1 (ESI; Figure S10a & b)**. In these two cases the colour of the **SA1** categorically became light yellow (**ESI; Figure S11**). Thus it was not possible to discriminate any single metal ion through **SA1** either by naked-eye change or by UV-visible spectral changes.

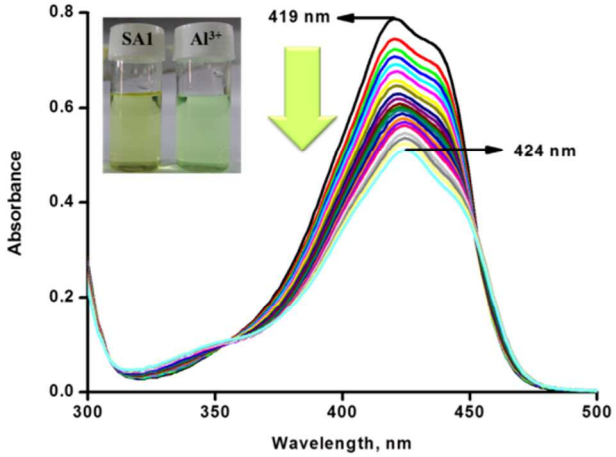

Fig. 5 UV-visible titration spectrum of 10 μM aqueous solution of SA1 with Al^{3+}

The non-selectivity of **SA1** towards a particular metal ion in UV-visible and naked–eye changes led us to check further the possibility of selectivity by modulating the emission spectral pattern of **SA1**. The fluorescence titration experiments were performed by gradually increasing Al^{3+} concentration into an aqueous solution of **SA1** (0.1 μM). The emission spectrum of free **SA1** showed a weak dual emission band with emission maxima positioned at 471 and 498 nm upon its excitation at 419 nm (Fig. 6). Receptors having a C=N group have been observed to be non-fluorescent due to rapid *cis–trans* isomerisation **[17a-b, 21]**. The weak fluorescent nature of the **SA1** may be a consequence of strong inter and intramolecular hydrogen bonding which may be hampering the availability of the lone pairs over nitrogen leading to hampering of PET and fast interconversion of *cis* and *trans* forms of **SA1**. The presence of inter and intramolecular hydrogen bonding in **SA1** are well illustrated through its XRD structure (Fig. 3). Here it is worth to mention that **SA2/SA3/SA4** having almost comparable structures with **SA1** even than they were non-fluorescent **[15,16a]** while **SA5** is weakly fluorescent **[16b]** only. Thus our structural tuning of **SA1** through introduction of DEA group further enhanced the hydrogen bonding ability of the same which ultimately affected availability of lone pair over N atom for PET and hence provided planarity and rigidity to **SA1** and finally became responsible for its weak fluorescent nature.

Upon concomitant additions of Al^{3+} (0-10 equiv.) to the **SA1** solution we got fully developed emission bands at 471 and 498 nm with ~8-fold fluorescence enhancement (Fig. 6). The observation of this type of dual emission bands for Al^{3+} is rare in literature. Most of the Al^{3+} responsive fluorescent receptors reported till now used to emit at a single wavelength only. Furthermore, upon separate respective additions of other metal ions to the **SA1**, no obvious fluorescence enhancement could be observed, indicating that this change was specific only for Al^{3+} (Fig.11). Moreover, the separate addition of 10 equiv. of $Al(NO_3)_3$ to the **SA1** gave rise to the similar emission profiles (**ESI; Figure S12**), indicating an almost negligible effect of the counter-anion on the recognition ability and photophysical properties of **SA1**.

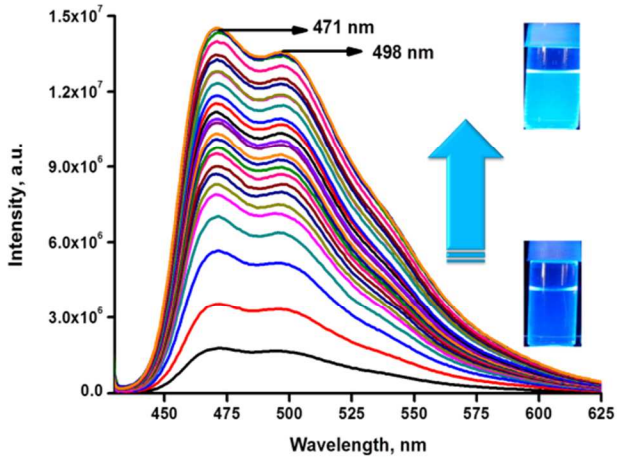

Fig. 6 Fluorescence titration profile of SA1 with Al^{3+} at 0.1 μM aqueous solution

For the selective fluorescent enhancement of **SA1** with Al^{3+} several factors can be listed to rationalize. The initial weak fluorescence of **SA1** may be due to the partial hampering of PET and *cis-trans* isomerization around C=N bond of **SA1** through intra and intermolecular hydrogen bondings. Upon the chelation of **SA1** by Al^{3+} the signal transduction occurs via chelation enhanced fluorescence (CHEF) process. The enhancement in fluorescence was assigned due to the binding of Al^{3+} with donor atoms of **SA1**, which ultimately led to cessation of PET and *cis-trans* isomerization around C=N bond. The hydroxyl group seems to play an important role in the recognition of the Al^{3+} by strengthening the CHEF and hence inhibiting the C=N isomerization and PET completely leading to fluorescence enhancement in the form of dual emission band. The dual emission at 471 and 498 nm is a consequence of the normal planar intramolecular charge transfer (PICT) state due to inhibition of C=N isomerization and twisted intramolecular charge transfer (TICT) state **[17a]** respectively due to presence of DEA group at **SA1**. Due to the absence of DEA pendant group over **SA2**, **SA3** and **SA5** those did not showed any such dual emission **[15,16b]**. However, **SA4** showed dual emission bands at 485 and 512 nm **[16a]** due to the presence of flexible –N atom able to show TICT state on the similar line of **SA1**.

Binding behaviour of Al^{3+} with SA1

The careful analysis of Job's plot (**ESI; Figure S13**) derived from the fluorescence titration experiment shows that **SA1** binds with Al^{3+} in 2:1 binding stoichiometry. The same was further confirmed by ESI MS of **SA1**-Al^{3+} complex (**ESI; Figure S8**) which showed a molecular ion peak m/z at 593.4 (Calcd. for $[2\mathbf{SA1}–2H+Al]^+$ = 593.28). The corresponding binding constant of **SA1** with Al^{3+} has been determined by non-linear fitting of fluorescence titration data using 2:1 binding equation **[22]**. The value of binding constant (c) was found to be 4050 $M^{-1/2}$ with a satisfactory correlation coefficient value (R^2 = 0.9898) (**ESI; Figure S14**). In the given equation **[22]** *'n'* is the number of Al^{3+} ions bound to each **SA1** (here n = 0.5). The value of '*n*' confirmed the 2:1 stoichiometry for the **SA1**–Al^{3+} complex.

Furthermore, the interaction of the hydroxyl groups of **SA1** with the Al^{3+} ion was supported by FTIR measurements (**ESI; Figure S3 & S7**). The distinctive absorption peak at 3435 cm^{-1}, ascribed to the characteristic stretching vibration band of the OH group of **SA1**, was marked at lower wavenumber at 3391 cm^{-1} for the **SA1**−Al^{3+} complex. Further new bands at 3110 cm^{-1} and 1635 cm^{-1} observed for –NH and >C=O stretching vibrations respectively in the complex which confirms the involvement of one of hydroxyl group in the process of keto-enol tautomerisation of **SA1** upon its complexation. Moreover the involvement of aldimine –N atom in binding was confirmed by its lowering in terms of wavenumber (from 1617 cm^{-1} to 1610 cm^{-1}) upon interaction of Al^{3+} with **SA1**. Thus IR studies clearly proved the involvement of OH, imine N-atom in binding with Al^{3+}.

For having further insight into the binding event of **SA1** with Al^{3+} we performed ^1H NMR titration experiment **(ESI; Figure S15)**. Significant spectral changes were observed upon addition of different aliquots of Al^{3+} (as its chloride salt) to the DMSO-d_6 solution of **SA1 (ESI; Figure S15)**. Further we compare the changes in chemical shifts of **SA1** protons with that of the ^1H NMR spectrum of the isolated **SA1**+ $AlCl_3$ complex DMSO-d_6 (Fig. 7).

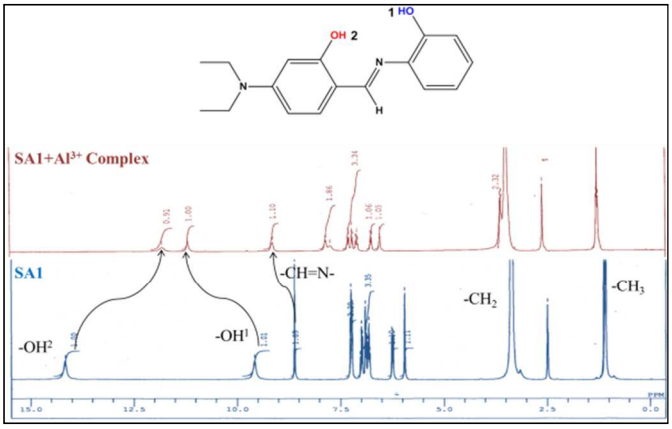

Fig. 7 ^1H NMR spectra of SA1 and its corresponding Al^{3+} complex in DMSO–d_6 solution

The $–OH^1$ (Fig. 7) along with aldimine protons (–CH=N–) showed remarkable downfield shifting from 9.583 to 11.021 δ ppm and 8.610 to 8.980 δ ppm respectively supporting the binding of the O and N atoms with Al^{3+}. Aromatic protons along with methyl and methylene protons also shifted marginally downfield upon Al^{3+} complexation. One interesting observation was that the $–OH^2$ proton experienced remarkable upfield shifting from 14.169 δ ppm to finally at 11.674 δ ppm. The same was assigned as the consequence of inter conversion of $–OH^2$ proton (Fig. 7) into –NH due to keto-amine tautomerisation of **SA1** upon its complexation with Al^{3+}. Overall changes in the chemical shifts of protons during titration with Al^{3+} clearly indicated N–atom of aldimine along with O1 and O2 (as keto) as the donor atoms in tridentate fashion. Besides the changes in the chemical shifts of **SA1** protons in the presence of Al^{3+} the corresponding ^{13}C NMR spectrum of the **SA1**+Al^{3+} complex also experienced appreciable changes in comparison to that of **SA1 (ESI; Figure S2 & S6)**.

Here it is worth to mention that the ESI mass spectrum of **SA1** +Al^{3+} complex showed a m/z peak at 593.4 (**ESI; Figure S8)**, which is 2 unit less than the mass calculated for ($2\mathbf{SA1}+Al^{3+}$). The same indicated deprotonation of one of the phenolic –OH (either 1 or 2) of **SA1**. While the ^1H NMR studies during the entire course of titration with Al^{3+} did not support this notion **(Fig. 7, ESI; Figure S15)**. To overcome this discrepancy between ^1H NMR and MS studies we developed the single crystals of **SA1**+Al^{3+} (Cl^-/NO_3^-) complex. To our surprise the XRD pattern of the same showed **SA1** bound with the corresponding counter anion (Cl^-/NO_3^-) of the Al^{3+} through aldimine N having H^+ rather than Al^{3+} (Fig. 8).

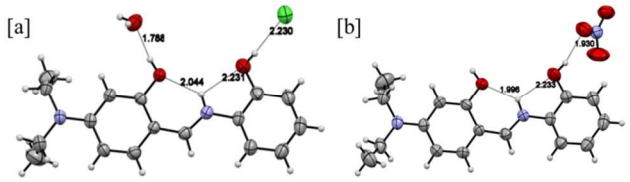

Fig. 8 Crystal structure of SA1 bound with (a) Cl^- and (b) NO_3^-

The crystal structure of protonated **SA1**–Cl^- also contained one hydrogen bonded water molecule with $–OH^2$ (1.788 Å) while no hydrogen bonded water molecule was found in the crystal structure of protonated **SA1**–NO_3^- (Fig. 8). The $–OH^1$---Cl^- and $–OH^1$---NO_3^- bond lengths were found to be 2.234 Å and 1.931 Å respectively. The corresponding crystal refinement data and structural parameters have been summarized in **ESI, Table 1**. Crystal packing of the protonated **SA1**+Cl^- complex is stabilized mainly by intermolecular hydrogen bonding interactions among **SA1**, water and Cl^- ions (Fig. 9a). The packing diagram of the protonated **SA1**+Cl^-/NO_3^- complexes along a, b and c-axis are shown in Fig. 9. The hydrogen bonded Cl^-/NO_3^- with protonated **SA1** further led a beautiful piece of supramolecular architecture shown in Fig. 10.

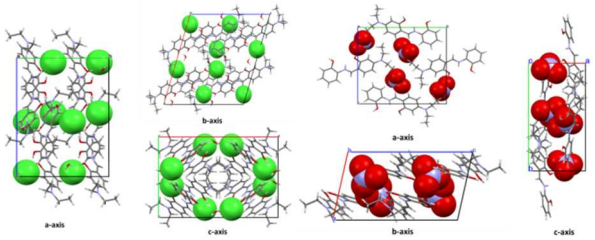

Fig. 9 Packing diagram of the protonated SA1+Cl^-/NO_3^- complexes along a, b and c-axis. Showing Cl^- and NO_3^- ions in space fill model

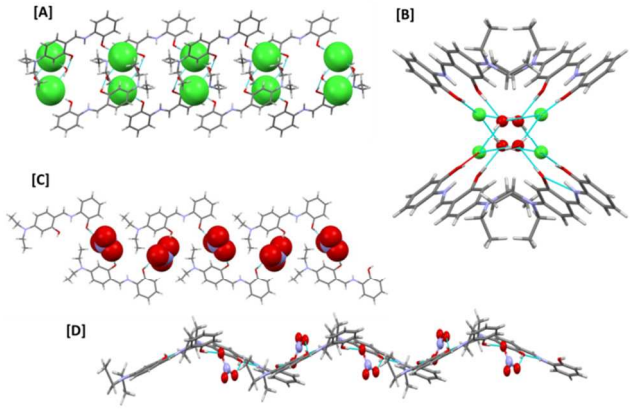

Fig. 10 Supramolecular architecture resulted from the inter and intra molecular hydrogen bonding between Cl^-/NO_3^- and protonated SA1 molecule; [A] and [B] for Cl^- ion, and [C] and [D] for NO_3^- ion

From the above crystallographic data it may be assumed that during crystallisation process the **SA1**+Al^{3+} complex underwent decomplexation due to the ongoing acid-base chemistry in aqueous solution as expressed with the help of following equation.

Hence H^+ ion generates through above reaction pathway and thus we observed protonated structures of **SA1** with the corresponding chloride and nitrate counter anions found in the unit cell. This type of substitution of Al^{3+} by H^+ can be understood in terms of much higher polarization power of H^+ as compared to Al^{3+}. Similar proposal of protonation of a pyrimidine–based Schiff base receptor was mooted out by us recently **[17a]** for explaining its selective *'on–off'* fluorescence switching in the presence of Al^{3+} and $HSO_4^-/H_2PO_4^-$ respectively. Here the $HSO_4^-/H_2PO_4^-$ ion served as a source of H^+ ion in aqueous medium thus we exploited the acidic character of $HSO_4^-/H_2PO_4^-$ for its selective sensing. To establish and justify the fact that it is the Al^{3+} and not the H^+ ion which was responsible for the fluorescence enhancement of the **SA1**, we recorded its fluorescence spectra in the presence of 5 equiv. of H^+ also but no observable fluorescence enhancement was marked as it was in the case of Al^{3+} (**ESI; Figure S16)**. However the emission spectrum of **SA1**+Al^{3+} complex was slightly quenched upon addition of 100 equiv. of H^+ (**ESI; Figure S16)**. Besides protonation Schiff bases are also quite prone towards hydrolysis in acidic medium in the presence of H^+ as well as through a few metal ions including Al^{3+} also as observed by us and other workers also **[23]**. The XRD and other spectroscopic studies under present study did not indicate hydrolysis of **SA1** in the presence of H^+/Al^{3+}.

Thus in the light of above XRD reports along with ^{1}H NMR titration the loss of one proton of $–OH^1$ (since other one i.e., $–OH^2$ got involved in keto-amine tautomerism) from **SA1** and ultimately loss of two protons from 2**SA1**+Al^{3+} have been rationalized. The binding of $–OH^1$ with Cl^-/NO_3^- through hydrogen bonding may be taken as responsible for significant downfield shifting of $–OH^1$ in ^{1}H NMR studies (Fig. 11). Hence this very proton underwent loss during the course of mass spectral studies of **SA1**+Al^{3+} complex.

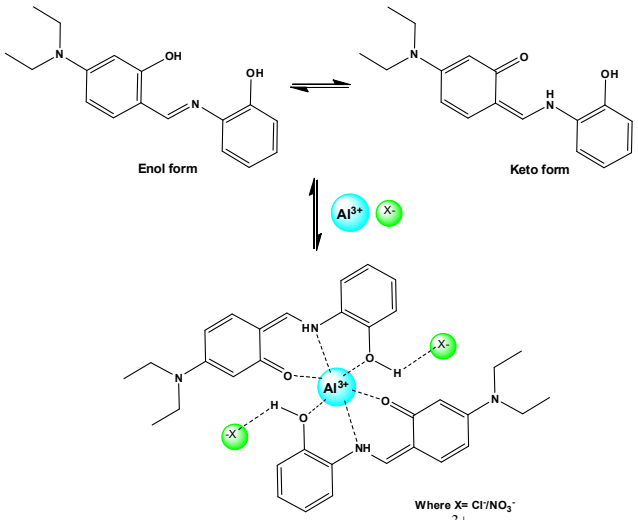

Fig. 11 Proposed binding mode of Al^{3+} with SA1

Based on the above facts, we proposed a rational coordinated mode in which Al^{3+} is hexa-coordinated with two tridentate ligand **SA1** having O2N type donor set (Fig. 11). The hexa-coordination of Al^{3+} is quite common for Al^{3+} sensors **[12a,d,e; 14c-g; 17c,e; 20a,c]**. On the basis of XRD, MS and ^{1}H NMR spectral studies the anionic moiety is shown as hydrogen bonded with $–OH^1$ proton of **SA1**. Although this binding of anion did not affect the optical modulation of **SA1** but MS and ^{1}H NMR spectra underwent some minor changes, as discussed above.

Following three mechanistic pathways have been explored by the various workers for the sensing and binding of Al^{3+} with a variety of fluorescent probes till now;

- **(a)** Direct binding of Al^{3+} with the donor atoms of the probe **[12-16, 17b]**
- **(b)** Chemodosimetric approach involving hydrolysis of the probe **[24]**
- **(c)** Counter effect of in situ generated H^+ ion/externally added H^+ on the sensing event of Al^{3+}– receptor complex. **[17a, 14c, 25]**

We have our contribution in each and every type [**17a-b, 23a**]. Present communication seems to involve **(a)** followed by **(c)**.

Selectivity and Detection limit of SA1 for Al^{3+}

The selectivity of **SA1** was verified with chloride salts of Na^+, Mg^{2+}, Al^{3+}, Ca^{2+}, Cr^{3+}, Mn^{2+}, Fe^{3+}, Co^{2+}, Ni^{2+}, Cu^{2+}, Zn^{2+}, Cd^{2+}, Hg^{2+}, Pb^{2+} and In^{3+} respectively in aqueous medium. The addition of 10 equiv. each of above mentioned alkali or alkaline earths or transition metal ions did not induce any discernible spectral changes in the emission spectrum of **SA1** (Fig. 12). However, the addition of Al^{3+} turned *'on'* the fluorescence intensity of **SA1** with dual channel emission bands at 471 and 498 nm. The selectivity of **SA1** for Al^{3+} over In^{3+}, Mn^{2+}, Fe^{3+} and Cu^{2+} is important because these metal ions generally interfere in the detection of Al^{3+} in their mixture. Interestingly the **SA1** performed well in the presence of these and other metal ions except in the case of Fe^{3+}/Cu^{2+} where we observed quenching.

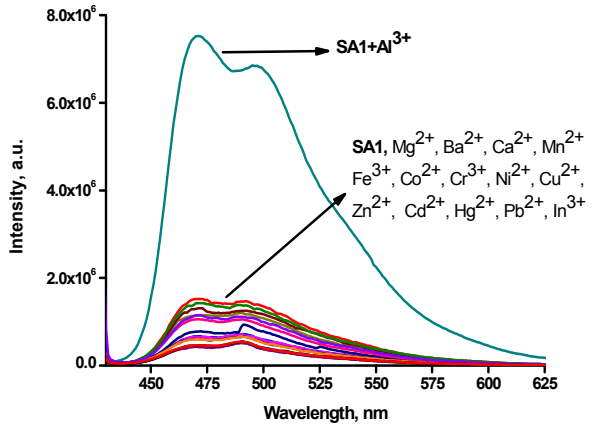

Fig. 12 Effects of various metal ions on the emission profile of SA1

The detection limit of **SA1** for Al^{3+} was calculated using fluorescence titration data according to the IUPAC definition **[26]** and same was found to be 2.73×10^{-9} M with a linearity range of 4.00×10^{-8} to 1.40×10^{-7} M for Al^{3+} **(ESI; Figure S17).** Although a number of probes for Al^{3+} are reported in the literature but only few of them were able to detect Al^{3+} in the aqueous environment with nano-molar detection ability **[12c, 17a-c, 19]**. The high sensitivity of **SA1** towards Al^{3+} may be understood in terms of introduction of hydrophobic group DEA which ultimately controls the strong hydration of Al^{3+} ion. Our previous report for Al^{3+} selective fluorescent probe also embodied DEA group and exhibited nano-molar sensitivity [**17b**].

pH Study

The fluorescence changes of **SA1** (0.5 μM) in the absence and presence of 10 equiv. of Al^{3+}, in different pH environments (1–13), were also studied **(ESI, Fig. S18)**. **SA1** fluoresces weakly between pH 4 and 10. However, upon addition of the Al^{3+}, a significant increase in the emission intensity of **SA1** recorded at 471 nm in the same pH range (4–10) was observed. Such broad pH spans in an aqueous medium make **SA1** very useful in several applications, such as Al^{3+} detection in wastewater, industrial analysis, and physiological treatment.

Cell imaging studies

A practical bio imaging application of **SA1** for Al^{3+} in biological samples was developed by confocal fluorescence microscopy on Nikon ECLIPSE-Ti confocal laser scanning microscopy. Under selective excitation of the **SA1** with longer-wavelength light at 488 nm, the staining LLC cells with a 50 μM solution of **SA1** for 24 h at 37 ºC led no observable intracellular fluorescence (Fig. 13A-C). The cells were then supplemented with 50 μM $Al(NO_3)_3$ in the growth medium loaded with **SA1** under the same conditions; a significant increase in the fluorescence from the intracellular area was observed (Fig. 13D-E**).** Bright-field measurements confirmed that the cells after treatment with Al^{3+} and **SA1** were viable throughout the imaging experiments. As depicted in Fig. 13F, the overlay of fluorescence and bright-field images reveals that the fluorescence signals are well localized in the cellular areas, indicating a subcellular distribution of Al^{3+} and good cell-membrane permeability of **SA1**.

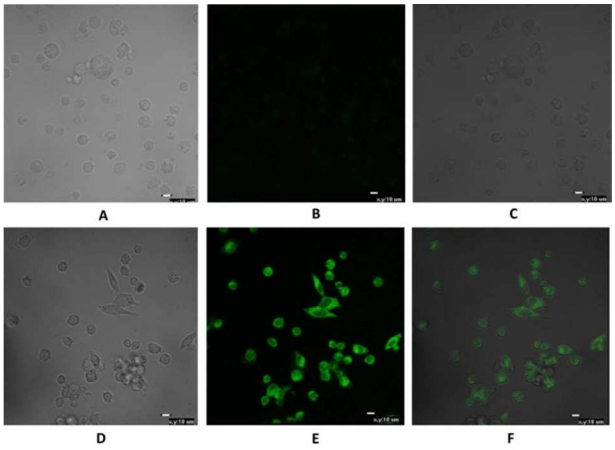

Bright field **488 nm** **Overlay**

Fig. 13 Representative fluorescence images of LLC cells; (A, B and C) cells incubated with 50 μM SA1 for 24 h; and (D, E and F) cells were incubated with SA1+Al^{3+} (λ_{ex} = 488 nm)

Conclusion

In summary, we have developed a new salicylimine-based Schiff base for selective fluorescent detection of Al^{3+} in aqueous medium. The simplicity, nano-molar sensitivity, water compatibility and cell permeability of **SA1** demonstrate the worth of the same in environmental and biological systems both. Through present research paper we explore how a simple modification over an existing probe enhances its performance upto a large extant. The hydrophobic nature of DEA group controls strong hydration of Al^{3+} in aqueous medium and consequently responded with high sensitivity with dual channel emission due to TICT state. Present study will definitely provide guidelines for the development of new optical probes for analytes with judicious modification of existing probes instead of designing the new ones. The cell imaging results further suggest that **SA1** is permeable to cell membrane and can detect intracellular Al^{3+} within living cells quite efficiently. Moreover the binding of protonated **SA1** with Cl^-/NO_3^- may further extend its functionality as a synthetic anion transporter and mimicking of a naturally occurring anion transporter *viz.,* prodigiosin. Detailed studies in the same context are underway in our laboratory.

Acknowledgements

Neeraj acknowledges UPE-JRF for research fellowship. VK is thankful to UGC, New Delhi for University Research Fellowships. RP and SKA are thankful to UGC and CSIR, New Delhi for Junior Research Fellowships respectively. A.K. acknowledges UGC, New Delhi for DSK Postdoctoral Fellowship [F.4-2/2006(BSR)/13-398/2011(BSR)]. Authors are thankful to Dr P. K. Roychowdhury, Director, Chembiotek Research International, Kolkata for providing mass spectral analysis.

References

1 **(a)** G. Aragay, J. Pons, A. Merkoci, *Chem. Rev.,* 2011, **111**, 3433. **(b)** D. T. Quang, J. S. Kim, *Chem. Rev.,* 2010, **110**, 6280. **(c)** H. N. Kim, W. X. Ren, J. S. Kim, Yoon, *J. Chem. Soc. Rev.,* 2012, **41**, 3210. **(d)** P. Jiang, Z. Guo, *Coord. Chem. Rev.,* 2004, **248**, 205.

2 M.I.S. Verissimo, Joao A.B.P. Oliveira, M. Teresa S.R. Gomes, *Sens. Actuators, B* 2006, **118**, 192.

3 **(a)** C. Exley, *J. Inorg. Biochem.* 2003, **97**, 1. **(b)** T.L. MacDonald, *Trends Biochem. Sci.* 1988, **13**, 15.

4 N. E. W. Alstad, B. M. Kjelsberg, L. A. Vøllestad, E. Lydersen, A. B. S. Poléo, *Environ. Pollut.,* 2005, **133**, 333.

5 R. J. P. Williams, *Coord. Chem. Rev*., 2002, **228**, 93

6 T. P. Flaten, *Brain Res. Bull*., 2001, **55**, 187.

7 **(a)** I.S. Parkinson, M.K. Ward, D.N.S. Kerr, *J Clin Pathol* 1981, **34**, 1285. **(b)** V. K. Gupta, A. K. Jain, G. Maheshwari, *Talanta* 2007, **72**, 1469.

8 Y. Jeong, J. Yoon, *Inorg. Chim. Acta*, 2012, **381**, 2.

9 K. Soroka, R. S. Vithanage, D. A. Phillips, B. Walker, P. K. Dasgupta, *Anal. Chem.,* 1987, **59**, 629.

10 S. Das, M. Dutta, D. Das, *Anal. Methods*, 2013, **5**, 6262 a*nd references therein*.

11 T. Keawwangchai, N. Morakot, B. Wanno, *J. Mol. Model*, 2013, **19**, 1435.

12 **(a)** D. Maity, T. Govindaraju, *Eur. J. Inorg. Chem.* 2011, 5479. **(b)** Y. Zhao, Z. Lin, H. Lia, C. Duan, Q. Meng, *Inorg. Chem. Commun.,* 2006, **9**, 966. **(c)** C. Gou, S.-H. Qin, H.-Q. Wu, Y. Wang, J. Luo, X.-Y Liu, *Inorg. Chem. Commun.,* 2011, **14**, 1622. **(d)** W. –H. Ding, W. Cao, X.-J. Zheng, D.-C. Fang, W.-T. Wong, L.-P. Jin, *Inorg. Chem.,* 2013, 52, 7320. **(e)** D. Karak, S. Lohar, A. Sahana, S. Guha, A. Banerjee, D. Das, *Anal. Methods*, 2012, **4**, 1906. **(f)** H. Xu, X. Tao, Y. Li, Y. Shen, Y. Wei, *Spectrochim. Acta, Part A*, 2012, **91**, 375.

13 Y.-W. Liu, C.-H. Chen, A.-T. Wu, *Analyst*, 2012, **137**, 5201.

14 **(a)** S. H. Kim, H. S. Choi, J. Kim, S. J. Lee, D. T. Quang, J. S. Kim, *Org. Lett.,* 2010, **12**, 560. **(b)** D. Maity, T. Govindaraju, *Chem. Commun.,* 2010, **46**, 4499. **(c)** X. Sun, Y.-W. Wang, Y. Peng, *Org. Lett.,* 2012, **14**, 3420. **(d)** W. Lin, L. Yuan, J. Feng, *Eur. J. Org. Chem.,* 2008, 3821. **(e)** A. B. Othman, J. W. Lee, Y. D. Huh, R. Abidi, J. S. Kim, J. Vicens, *Tetrahedron*, 2007, **63**, 10793. **(f)** Y.-W. Wang, M.-X. Yu, Y.-H. Yu, Z.-P. Bai, Z. Shen, F.-Y. Li, X.-Z. You, *Tet. Lett.*, 2009, **50**, 6169. **(g)** D. Maity, T. Govindaraju, *Inorg. Chem.*, 2010, **49**, 7229. **(h)** T. Han, X. Feng, B. Tong, J. Shi, L. Chen, J. Zhic, Y. Dong, *Chem. Commun*., 2012, **48**, 416.

15 S. Kim, J. Y. Noh, K. Y. Kim, J. H. Kim, H. K. Kang, S.-W. Nam, S. H. Kim, S. Park, C. Kim, J. Kim, *Inorg. Chem.*, 2012, **51**, 3597. **(b)** R. Kang, X. Shao, F. Peng, Y. Zhang, G.-T. Sun, W. Zhao, X.-D. Jiang, *RSC Adv.*, 2013, **3**, 21033.

16 H. J. Jung, N. Singh, D. Y. Lee, D. O. Jang, *Tet. Lett.*, 2009, **50**, 5555.

17 **(a)** A. Kumar, V. Kumar, K. K. Upadhyay, *Analyst*, 2013, **138**, 1891. **(b)** K. K. Upadhyay, A. Kumar, *Org. Biomol. Chem.*, 2010, **8**, 4892. **(c)** A. Sahana, A. Banerjee, S. Lohar, B. Sarkar, S. K. Mukhopadhyay, D. Das, *Inorg. Chem.,* 2013, **52**, 3627. **(d)** T.-H. Ma, M. Dong, Y.-M. Dong, Y.-W. Wang, Y. Peng, Chem. Eur. J. 2010, **16**, 10313.

18 **(a)** J. Y. Noh, S. I. Kim, H. Hwang, G.Y. Lee, J. Kang, S. H. Kim, J. Min, S. Park, C. Kim, J. Kim, *Dyes and Pigments* 2013, **99**, 1016. **(b)** Y. K. Jang, U. C. Nama, Lim, H. Kwon, I. H. Hwang, C. Kim, *Dyes and Pigments* 2013, **99**, 6.

19 L. Wang, W. Qin, X. Tang, W. Dou, W. Liu, Q. Teng, X. Yao, *Org. Biomol. Chem*., 2010, **8**, 3751.

20 **(a)** H. M. Park, B. N. Oh, J. H. Kim, W. Qiong, I. H. Hwang, K.-D. Jung, C. Kim, J. Kim, *Tet. Lett.* 2011, **52**, 5581. **(b)** Y. J. Jang, Y. H. Yeon, H. Y. Yang, J. Y. Noh, I. H. Hwang, C. Kim, *Inorg. Chem. Commun.* 2013, **33**, 48. **(c)** S. Das, A. Sahana, A. Banerjee, S. Lohar, D. A. Safin, M. G. Babashkina, M. Bolte, Y. Garcia, I. Hauli, S. K. Mukhopadhyay, D. Das, *Dalton Trans.*, 2013, **42**, 4757.

21 J.-S. Wu, W.-M. Liu, X.-Q. Zhuang, F. Wang, P.-F. Wang, S.-L. Tao, Zhang, X.-H., S.-K., Wu, S.-T. Lee, *Org. Lett.*, 2007, **9**, 33.

22 C. R. Lohani, J.-M. Kim, S.-Y. Chung, J. Yoon, K.-H., Lee, *Analyst*, 2010, **135**, 2079.

23 **(a)** V. Kumar, A. Kumar, U. Diwan, K. K. Upadhyay, *Chem. Commun.,* 2012, **48**, 9540. **(b)** J. H. Kim, H. J. Kim, C. W. Bae, J. W. Park, J. H. Lee, J. S. Kim, *Arkivoc*, 2010, 170. **(c)** H. S. Jung, J. H. Han, Z. H. Kim, C. Kang, J. S. Kim, *Org. Lett.*, 2011, **13**, 5056. **(d)** M. H. Lee, T. V. Giap, S. H. Kim, Y. H. Lee, C. Kang, J. S. Kim, *Chem. Commun.*, 2010, **46**, 1407. **(e)** H. S. Jung, J. H. Han, Y. Habata, C. Kang, J. S. Kim, *Chem. Commun.*, 2011, **47**, 5142. **(f)** A. K. Gupta, A. Dhir, C. P. Pradeep, *Dalton Trans.,* 2013, 2013**, 42,** 12819**.**

24 A. Helal, S.H. Kim, H.-S. Kim, *Tetrahedron*, 2013, **69**, 6095.

25 Y. Lu, S. Huang, Y. Liu, S. He, L. Zhao, X. Zeng, *Org. Lett.,* 2011, **13**, 5274.

26 **(a)** IUPAC, *Spectrochim. Acta Part B*, 1978, **33**, p. 242. **(b)** USEPA, Appendix B to Part 136-Definition and Procedure for the Determination of the Method Detection Limit- Revision 1.11, Federal Register 49 (209), 43430, October 26, 1984. Also referred to as "40 CFR Part136".

A remarkable effect of *N*,*N*-diethylamino functionality on the optoelectronic properties of a salicylimine-based probe for Al^{3+}

Neeraj, [‡1]Ajit Kumar,[‡1] Virendra Kumar,[1] Rahul Prajapati,[1] Sharad Kumar Asthana,[1] K. K. Upadhyay,[1*] Jianzhang Zhao[2]

[1]Department of Chemistry (Centre of Advanced Study), Faculty of Science, Banaras Hindu University, Varanasi, Uttar Pradesh-221005, India

[2]State Key Laboratory of Fine Chemicals, Dalian University of Technology, Dalian 116012, China

***E-mail:** drkaushalbhu@yahoo.co.in; kku@bhu.ac.in; **Tel:** +91 542-6702488

‡These authors contributed equally to this work.

A new live-cell permeable, fluorescent probe comprised of a simple salicylimine-based Schiff base (**SA1**) has been developed for Al^{3+} with nano-molar sensitivity in aqueous medium. The incorporation of *N*,*N*-diethylamino (**DEA**) group as a fine controllable unit affects the functionality of **SA1** remarkably in terms of its sensitivity, water compatibility, efficiency as well as its mechanistic aspect.